UNSTABLE SEEPAGE LAW OF LOW PERMEABILITY DOUBLE DEFORMABLE MEDIUM RESERVOIR

Wang Meinan, Zhang Junting, Zhang Hongyou, Long Ming & Chen Xiaoqi
Bohai Oilfield Research Institute of CNOOC Ltd.-Tianjin Branch, Tang Gu
Tianjin 300459, **CHINA**

ABSTRACT

Based on the starting pressure gradient and double Deformable Medium of the fractured low permeability reservoir, the influence of the quadratic gradient term and deformable media on the filtration equation was considered, unsteady seepage mathematical model of low permeability double deformable medium reservoir was built, which was solved by finite difference method. The correlated pressure dynamic curve was drawn, unstable seepage law was analyzed. The results of the study show that, The influence of starting pressure gradient and deformation on the pressure characteristic curve is mainly manifested in the late period. The bigger the value was, the greater the range of the pressure and the pressure derivative curves going up was. The parameters for the characterization of double medium were interporosity-flow coefficient and elastic storage ratio. The bigger the interporosity-flow coefficient was, the time of "concave" appearance was earlier; The smaller the elastic storage ratio was, the width and depth of the "concave" was bigger.

Keywords: Low permeability reservoir; dual porosity media; deformable media; interporosity-flow coefficient; elastic storage ratio.

INTRODUCTION

With the continuous improvement of oil exploration and utilization, low permeability reserves have accounted for an increasingly large proportion. Under the current circumstance of this stressful oil reserve, how to utilize and develop low permeability oil reserves and improve development efficiency has significantly practical meaning to the sustainable and stable development of China's oil industry. The development of low permeable oilfield was closely related with fractures, compared with the conventional oil reservoirs, the productivity in the fractures of oil reservoirs and the matrix were complicated and diversified, how to calculate, forecast and the analyze the productivity of fractures and matrix was an important task for the low permeability oilfield development. Many laboratory experiments and field development show that, only the starting pressure gradient has been overcome can percolation flow in low permeability reservoir occur: Besides, the primitive permeability and porosity are very low in the exploitation and the relative range of variation of the permeability and porosity will have great effect. As a result, it is necessary to consider the influence of the deformation of the media. Unlike conventional reservoirs, fractured reservoirs have typical characters of dual-porosity, the fluid flows between matrix and fracture. From physical meaning and basic characteristics of the low permeability reservoir seepage process, the quadratic gradient term, the deformation of the media and the dual-porosity characters was considered, the seepage model of the dual-porosity oil reservoir model with low permeability was established, the seepage law of the dual-porosity oil reservoir model with low permeability was analyzed.

1. Establishment of Nonlinear Seepage Equation

(1)Assumptions

a. Fluid is slightly compressible;

b. The gravity and capillary force can be ignored;

c. The output of the well is q and thickness of the reservoir is uniform;

d. The flow through the wellbore is the result of fracture, matrix as the source;

e. Fluid flow is single-phase laminar (follow non-Darcy flow law with starting pressure gradient);

f. The porosity of each medium (fracture or matrix) is independent of the pressure change with another medium;

g. The reservoir is homogeneous and isotropic, with infinite lateral extension and closed top and bottom border;

h. The medium is slightly compressible and compression coefficient is constant. But the compression can cause significant changes in the permeability of the formation.

For the mathematical description of fractured reservoirs, we use two single-phase system - overlay of fracture and matrix to indicate that the space has two pressure at each point: average fluid pressure of the fracture p_f and average fluid pressure of the matrix p_m(Figure 1).

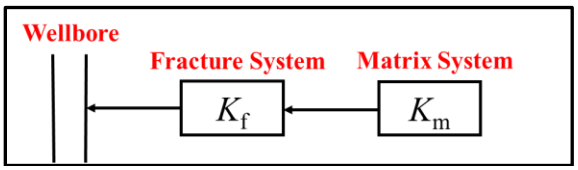

Figure 1 Physical model for fractured reservoir

(2)Continuity Equation

Considering single-phase fluid flow whose porosity is Φ in porous medium, radial flow continuity equation is obtained by principle of mass conservation:

Continuity equation of fracture system:

$$-\frac{1}{r}\cdot\frac{\partial}{\partial r}(\rho r v_r)+q^*=\frac{\partial}{\partial t}(\varphi_f\rho) \qquad (1)$$

Continuity equation of matrix system:

$$-q^*=\frac{\partial}{\partial t}(\varphi_m\rho) \qquad (2)$$

Interporosity flow equation:

$$q^*=\frac{\alpha\rho K_m}{\mu}(p_m-p_f) \qquad (3)$$

(3)Constitutive Equation:

The medium and the fluid were slightly compressible and the compressibility was constant. We can get state equation：

For compressible fluid:

$$\rho=\rho_0 e^{C_\rho(p-p_0)} \qquad (4)$$

For compressible porous medium:

$$\phi=\phi_0 e^{C_\phi(p-p_0)} \qquad (5)$$

$$K=K_0 e^{\gamma(p-p_0)} \qquad (6)$$

(4)Momentum Equation:

The fluid of low permeability reservoirs will have to surmount the starting pressure gradient to flow. So in order to adequately describe the rule of starting pressure, we take the following methods to describe the fluid flow process:

$$\begin{cases} v = 0, \dfrac{\Delta p}{L} \le G \\ v = \dfrac{K}{\mu}\left(\dfrac{\Delta p}{L} - G\right), \dfrac{\Delta p}{L} > G \end{cases} \tag{7}$$

The momentum equation and constitutive equation were substituted into the continuity equation of fracture system and matrix system (Assuming: $\gamma >> C_{\mathrm{Lf}}$) to obtain flow equation:

$$\frac{\partial^2 p_{\mathrm{f}}}{\partial r^2} + \gamma\left(\frac{\partial p_{\mathrm{f}}}{\partial r}\right)^2 + \left[\frac{1}{r} - \gamma \cdot G\right] \cdot \frac{\partial p_f}{\partial r} - \frac{G}{r} = \frac{\mu}{K_{\mathrm{f}}}\left(\phi_{\mathrm{f}} C_{\mathrm{t1}} \frac{\partial p_{\mathrm{f}}}{\partial t} + \phi_{\mathrm{m}} C_{\mathrm{t2}} \frac{\partial p_{\mathrm{m}}}{\partial t}\right) \tag{8}$$

$$\varphi_{\mathrm{m}} C_{\mathrm{t2}} \frac{\partial p_{\mathrm{m}}}{\partial t} = \frac{\alpha K_{\mathrm{m}}}{\mu}\left(p_{\mathrm{f}} - p_{\mathrm{m}}\right) \tag{9}$$

Where $C_{\mathrm{Lf}} = \dfrac{1}{\rho}\dfrac{\partial \rho}{\partial p_{\mathrm{f}}}$, $C_{\mathrm{Lm}} = \dfrac{1}{\rho}\dfrac{\partial \rho}{\partial p_{\mathrm{m}}}$, $C_{\varphi \mathrm{f}} = \dfrac{1}{\varphi_{\mathrm{f}}}\dfrac{\partial \varphi_{\mathrm{f}}}{\partial p_{\mathrm{f}}}$, $C_{\varphi \mathrm{m}} = \dfrac{1}{\varphi_{\mathrm{m}}}\dfrac{\partial \varphi_{\mathrm{m}}}{\partial p_{\mathrm{m}}}$, $C_{\mathrm{t1}} = C_{\varphi \mathrm{f}} + C_{\mathrm{Lf}}$, $C_{\mathrm{t2}} = C_{\varphi \mathrm{m}} + C_{\mathrm{Lm}}$

2. Transformation of the Model

(1) Dimensionless variable of model

$$\frac{\partial^2 p_{\mathrm{Df}}}{\partial r_{\mathrm{D}}^{\,2}} - \beta\left(\frac{\partial p_{\mathrm{Df}}}{\partial r_{\mathrm{D}}}\right)^2 + \left(\frac{1}{r_{\mathrm{D}}} - B\beta\right)\frac{\partial p_{\mathrm{Df}}}{\partial t_{\mathrm{D}}} + \frac{B}{r_{\mathrm{D}}} = \omega\frac{\partial p_{\mathrm{Df}}}{\partial t_{\mathrm{D}}} + (1-\omega)\frac{\partial p_{\mathrm{Dm}}}{\partial t_{\mathrm{D}}} \tag{10}$$

$$(1-w)\frac{\partial p_{\mathrm{Dm}}}{\partial t_{\mathrm{D}}} = \lambda\left(p_{\mathrm{Df}} - p_{\mathrm{Dm}}\right) \tag{11}$$

Where, $p_{\mathrm{Df}} = \dfrac{2\pi h K_0}{\mu q}\left(p_0 - p_{\mathrm{f}}\right)$, $p_{\mathrm{Dm}} = \dfrac{2\pi h K_0}{\mu q}\left(p_0 - p_{\mathrm{m}}\right)$, $r_{\mathrm{D}} = \dfrac{r}{r_{\mathrm{w}}}$, $\lambda = \dfrac{K_{\mathrm{m}} r_{\mathrm{w}}^{\,2}}{K_{\mathrm{f}}}\alpha$,

$t_{\mathrm{D}} = \dfrac{t K_0}{\mu\left(\varphi_{\mathrm{f}} C_{\mathrm{t1}} + \varphi_{\mathrm{m}} C_{\mathrm{t2}}\right) r_{\mathrm{w}}^{\,2}}$, $\beta = C_{\rho}(p_{\mathrm{i}} - p_{\mathrm{w}})$, $\gamma_{\mathrm{D}} = \dfrac{\mu q \gamma}{2\pi h K_0}$, $B = \dfrac{2\pi h K_0}{\mu q} G$, $\omega = \dfrac{\varphi_{\mathrm{f}} C_{\mathrm{t1}}}{\varphi_{\mathrm{f}} C_{\mathrm{t1}} + \phi_{\mathrm{m}} C_{\mathrm{t2}}}$

(2) Linearization of the model

The resulting model contains quadratic gradient term, we can use the Laplace transform to handle this problem.

$$p_{\mathrm{Df}} = -\frac{1}{\beta}\ln\left[1 - \beta\eta\left(r_{\mathrm{D}}, t_{\mathrm{D}}\right)\right] \ , \ p_{\mathrm{Dm}} = \xi\left(r_{\mathrm{D}}, t_{\mathrm{D}}\right) \ , \ x = \ln r_{\mathrm{D}} \tag{12}$$

Substituting the above equation into (3-20) and (3-21), the transformed flow equation is:

$$\frac{\partial^2 \eta}{\partial x^2} - B\beta e^x \frac{\partial \eta}{\partial x} + e^x B(1-\beta\eta) = \omega e^{2x}\frac{\partial \eta}{\partial t_{\mathrm{D}}} + (1-\omega)e^{2x}(1-\beta\eta)\frac{\partial \xi}{\partial t_{\mathrm{D}}} \tag{13}$$

$$(1-\omega)\frac{\partial \xi}{\partial \Delta t_{\mathrm{D}}} = \lambda\left[-\frac{1}{\beta}\ln(1-\beta\eta) - \xi\right] \tag{14}$$

By formula (12), when $p_{\mathrm{D}} = 0$, $\eta = 0$, $\xi = 0$, the initial condition is:

$$\eta\big|_{t_{\mathrm{D}}=0} = \xi\big|_{t_{\mathrm{D}}=0} = 0 \tag{15}$$

Internal boundary condition:

$$\frac{\partial \eta}{\partial x}\big|_{x=0} = -\left[(1-\beta\eta)^{-\frac{\gamma_{\mathrm{D}}}{\beta}} + B\right](1-\beta\eta) \tag{16}$$

Outer boundary condition:

$$\left.\frac{\partial \eta}{\partial x}\right|_{x=\ln\frac{r_e}{r_w}}=0 \quad (17)$$

$$\left.\eta\right|_{x=\ln\frac{r_e}{r_w}}=0 \quad (18)$$

$$\lim_{x\to\infty}\eta\left(x,t_D\right)=\lim_{x\to\infty}\xi\left(x,t_D\right)=0 \quad (19)$$

After the conversion, the quadratic gradient term is absorbed into the equation without making any approximation. Coefficients of nonlinear terms in the equation only restrict to the right side.

3. The solution of the model

The model is nonlinear problem with no analytical solution, the following uses numerical methods. We utilize implicit difference scheme for the numerical solution of the model, namely, the use of $\eta(x, t_D)$ and $\xi(x, t_D)$ on a first-order backward difference with respect to t_D and second-order difference with respect to x, write the differential form of equation (13) and (14):

$$\frac{\eta_{i+1}^{n+1}-2\eta_i^{n+1}+\eta_{i-1}^{n+1}}{\Delta x^2}-B\beta e^{i\cdot\Delta x}\frac{\eta_{i+1}^{n+1}-\eta_i^{n+1}}{\Delta x}+Be^{i\cdot\Delta x}\left(1-\beta\eta_i^{n+1}\right)=\omega e^{2i\cdot\Delta x}\frac{\eta_{i+1}^{n+1}-\eta_i^{n}}{\Delta t_D}+(1-\omega)e^{2i\cdot\Delta x}\left(1-\beta\eta_i^{n}\right)\frac{\xi_i^{n+1}-\xi_i^{n}}{\Delta t_D} \quad (20)$$

$$(1-\omega)\frac{\xi_i^{n+1}-\xi_i^{n}}{\Delta t_D}=\lambda\left[-\frac{1}{\beta}\ln\left(1-\beta\eta_i^{n}\right)-\xi_i^{n}\right] \quad (21)$$

Organize and simplify,

$$c(i)\eta_{i-1}^{n+1}+a(i)\eta_i^{n+1}+b(i)\eta_{i+1}^{n+1}=d(i) \quad (22)$$

$$\xi_i^{n+1}=e(i)\xi_i^{n}+f(i) \quad (23)$$

Where: $c(i)=1$, $a(i)=-2+B\beta e^{i\cdot\Delta x}\Delta x-B\beta e^{i\cdot\Delta x}\Delta x^2-\frac{\omega e^{2i\cdot\Delta x}\Delta x^2}{\Delta t_D}$, $b(i)=1-B\beta e^{i\cdot\Delta x}\Delta x$,

$$d(i)=\left[-\frac{\omega e^{2i\cdot\Delta x}\Delta x^2}{\Delta t_D}-(1-\omega)\beta e^{2i\cdot\Delta x}\Delta x^2\frac{\xi_i^{n+1}-\xi_i^{n}}{\Delta t_D}\right]\eta_i^{n}+\left[(1-\omega)e^{2i\cdot\Delta x}\Delta x^2\frac{\xi_i^{n+1}-\xi_i^{n}}{\Delta t_D}-e^{i\cdot\Delta x}B\Delta x^2\right],\quad e(i)=1-\frac{\lambda\Delta t_D}{1-\omega},$$

$$f(i)=-\frac{\lambda\Delta t_D}{\beta(1-\omega)}\ln\left(1-\beta\eta_i^{n}\right).$$

The difference scheme of closed outer boundary and constant production inner boundary:

$$\left.\frac{\partial \eta}{\partial x}\right|_{x=\ln\frac{r_e}{r_w}}=0 \quad (24)$$

$$\left.\frac{\partial \eta}{\partial x}\right|_{x=0}=-\left[\left(1-\beta\eta\right)^{-\frac{\gamma_D}{\beta}}+B\right]\left(1-\beta\eta\right) \quad (25)$$

By equation (24), we have:

$$-\eta_{n-1}+\eta_n=0 \quad (26)$$

By equation (25), we have:

$$-\eta_0+\eta_1=d_0 \quad (27)$$

Where, $d_0=-\left[\left(1-\beta\eta\right)^{-\frac{\gamma_D}{\beta}}+B\right]\left(1-\beta\eta\right)\Delta x$.

For n = 1, 2, ..., n-1 into equation (3-41), tridiagonal coefficient matrix equation can be obtained:

$$\begin{array}{l} i=0 \\ i=1 \\ i=2 \\ \cdots \\ i=n\text{-}1 \\ i=n \end{array} \begin{pmatrix} -1 & 1 & & & & \\ c(1) & a(1) & b(1) & & & \\ & c(2) & a(2) & b(2) & & \\ & & \cdots & \cdots & \cdots & \\ & & & c(n-1) & a(n-1) & b(n-1) \\ & & & & -1 & 1 \end{pmatrix} \begin{pmatrix} \eta_0 \\ \eta_1 \\ \eta_2 \\ \cdots \\ \eta_{n-1} \\ \eta_n \end{pmatrix} = \begin{pmatrix} d_0 \\ d_1 \\ d_2 \\ \cdots \\ d_{n-1} \\ d_n \end{pmatrix} \quad (28)$$

Tridiagonal coefficient matrix is a square matrix of order n+1, unknown number is $\eta_0, \eta_1, \ldots \eta_{n-1}, \eta_n$

By substituting the initial conditions of difference format into the difference format of flow equations, we will have three diagonal equations of order N. Every moment we can list the coefficient matrix, and based on each grid pressure value of moment n, we can use Thomas algorithm to solve pressure distribution of the next moment (n+1 moment), and so on…

4. Analysis of Seepage Law on Low Permeability Dual Deformable Media Reservoir

This chapter applies the percolation mathematical model of low permeability dual deformable media reservoir obtains the simulation results. With the results, we study the regulation of boundary motion at the condition of closed outer boundary and fixed-output inner boundary, draw the pressure dynamic curve of deformable media reservoir, analyze the effect of the parameters on the dynamic pressure.

4.1 Pressure Analysis on Low Permeability Dual Deformable Media Reservoir

Basic parameters of a low permeability reservoir are all in table1:

Table1 Basic parameters of a low permeability reservoir

K_f(μm^2)	100.0×10^{-3}	G(MPa/m)	0.05	h(m)	3
K_m(μm^2)	1×10^{-3}	γ(1/MPa)	0.04	r_w(m)	0.1
Φ_f	0.25	α	10	p_i(MPa)	16.5
Φ_m	0.65	C_{t1}(1/MPa)	0.33×10^{-15}	q(m^3/d)	3
μ(mPa•s)	6.8	C_{t2}(1/MPa)	3.3×10^{-15}	C_D	1
ρ(g/cm^3)	0.78	C_{lf}(1/MPa)	3.09×10^{-15}	S	2

From the above paraeters, we obtain the typical testing curve, as figure 2：

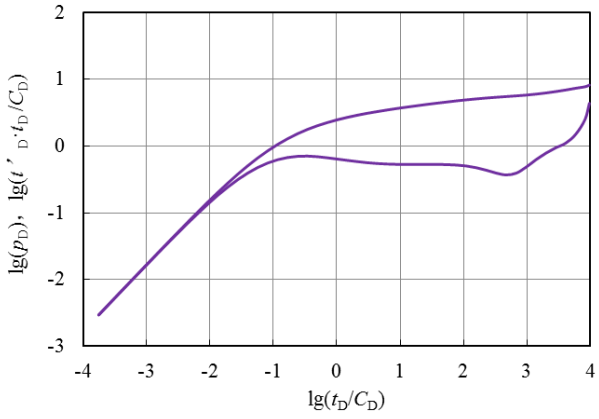

Figure 2 pressure dynamic testing curve

From the typical pressure dynamic curve, we can see that the log-log graph can be divided into five different stages. The first stage is the wellbore storage stage, the pressure cure and the derivative cure present a straight line with the slope of 45°. The second stage is the transitional stage, the derivative cure presents a hump. It reflects the situation of the near wellbore reservoir affected by the skin effect. The third stage is Fracture system radial flow stage, the fracture system flow reached a stage of radial flow, the pressure derivative changed along the horizontal line, and pressure rises continuously. The forth stage is Quasi-steady stage between medias, the flow from matrix system to fracture system, also known as flow between media, reflecting the channeling characteristics of transition zone fluid. Pressure becomes stable from the original, and then turns up. Therefore, at this stage the pressure derivative curve declines and then backs up, forming a "concave". The fifth stage is Radial flow stage of the whole system--late stage of the flow. The curve with different boundary value shows different trend. In the case of closed boundary, late stage curve occurs upturned.

4.2 The Effect of Wellbore Storage Coefficient and Skin Factor

Figure 3 indicates the effect of wellbore storage coefficient on the pressure dynamic curve. The wellbore storage coefficient has main effect on the first stage of the flow. As the dimensionless wellbore storage coefficient C_D increases (C_D=0.1, 1.0, 2.0), the early pressure curve is still a straight line with the slope of 1, but wellbore storage stage becomes longer; radial flow stage of fracture system is gradually being covered up, but still presents characteristics of dual media reservoir (Pseudo-steady stage between media).

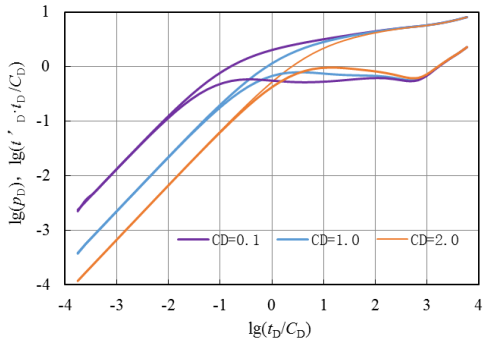

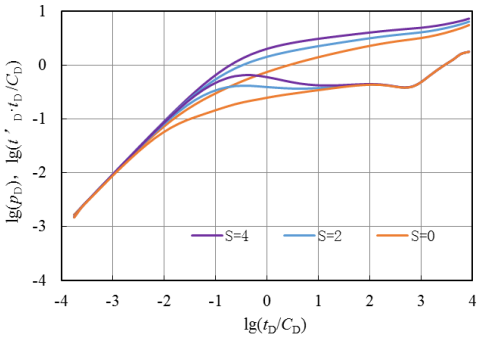

Figure 3 Influence of C_D on pressure curve **Figure 4 Influence of S on pressure curve**

Figure 4 indicates the effect of skin factor on the pressure dynamic curve. Skin factor has main effect on the second stage of the flow. As the skin factor S increases (S =0, 2, 4), the pressure curve of double logarithmic graph is also constantly on the move, while the "hump" of the pressure derivative curve is also on the rise.

4.3 The Effect of Medium Deformation and Starting Pressure Gradient

Figure 5 indicates the effect of medium deformation on the pressure dynamic curve. The medium deformation has main effect on the later stage of the flow. At the initial stage, there is a slow rise in pressure. The value of γ_D has little effect on the progress. After the initial stage, with the increase of time, pressure curves are divergent. The influence of γ_D on pressure is increasing, and dimensionless pressure increases with the value of γ_D reduces. Along with the increasing of the deformation medium elasticity, the pressure declines more rapidly. The emergence of "concave" is not dependent on γ_D. We can see that the curves obviously go upturn on the later period,which present the characteristics of closed boundary.

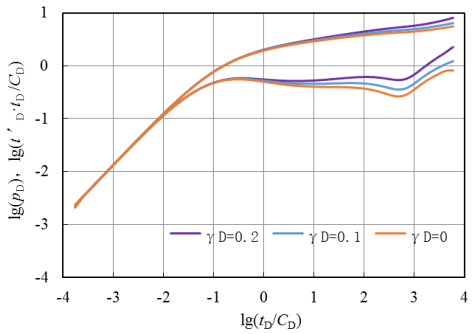

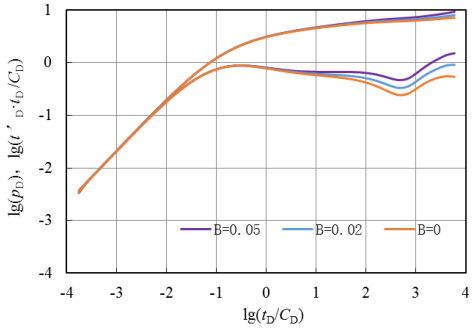

Figure 5 Influence of γ_D on pressure curve **Figure 6 Influence of *B* on pressure curve**

Figure 6 indicates the effect of starting pressure gradient on the pressure dynamic curve. The starting pressure gradient has main effect on the later stage of the flow. From the figure, we know that the various value of *B* makes the whole flow progress different and the starting pressure gradient has little influence on the initial stage. With the increase of time, pressure curves are divergent and the influence of *B* on pressure is increasing. The larger *B* is, the larger dimensionless pressure is, the earlier the curve upward, and the greater the upward amplitude is. The emergence of "concave" is not dependent on *B*. The existence of starting pressure makes the pressure curve go up. The greater the starting pressure gradient, the bigger the greater the upward amplitude, which is a feature of low permeability reservoir.

4.4 The Effect of Interporosity Flow Coefficient and Elastic Storage Ratio

Figure 7 indicates the effect of interporosity flow coefficient on the pressure dynamic curve. The interporosity flow coefficient has main effect on the later stage of the flow. It can be seen from the figure that λ determines the appearance time and location of "concave", the smaller the λ, the later the appearance time of "concave", the righter the "concave". The initial stage of pressure does not depend on λ.

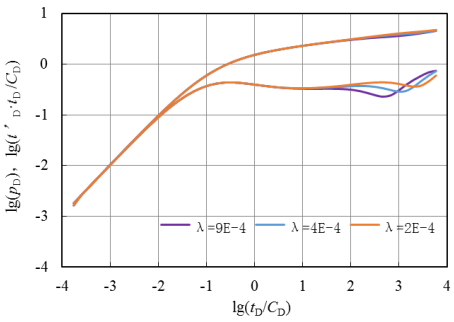

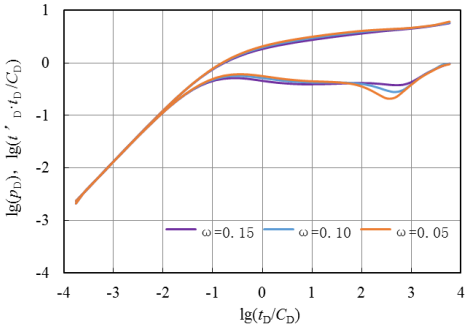

Figure 7 Influence of λ on pressure curve **Figure 8 Influence of ω on pressure curve**

Figure 8 indicates the effect of elastic storage ratio on the pressure dynamic curve. The elastic storage ratio has main effect on the later stage of the flow. As can be seen from the graph, ω determines the width and depth of concave of pressure derivative curve channeling stage. The smaller the ω, the longer the channeling stage, the wider and deeper the "concave". In the late stage, the pressure is not dependent on ω.

5.Conclusions

(1)The quadratic gradient term, the deformation of the media and the dual-porosity characters was considered, the seepage model of the dual-porosity oil reservoir model with low permeability was established, which was simplified by Laplace transform and solved by Finite difference method. The seepage law of the dual-porosity oil reservoir model with low permeability was analyzed.

(2)As the dimensionless wellbore storage coefficient increases, the early pressure curve is still a straight line with the slope of 1, but wellbore storage stage becomes longer. With the skin factor increasing, the pressure curve of double logarithmic graph is also constantly on the move, while the "hump" of the pressure derivative curve is also on the rise.

(3) The influence of starting pressure gradient and deformation on the pressure characteristic curve is mainly manifested in the late period. The smaller the value, the greater the dimension pressure difference later, namely, the faster the formation pressure drops. The effect will be more obvious if the two factors exist at the same time.

(4) Interporosity flow coefficient determines the appearance time and location of "concave". The smaller the value, the later the appearance time of "concave", the righter the "concave". Elastic storage ratio determines the width and depth of concave of pressure derivative curve channeling stage. The smaller the value, the longer the channeling stage, the wider and deeper the "concave".

6.Sign annotation

r——distance from the well, m; ρ——density, g/cm^3; v——Seepage velocity, cm/s; φ_f —— fracture porosity, %; φ_m——matrix porosity, %; K_f——fracture Permeability, $10^{-3}\mu m^2$; K_m—— matrix Permeability, $10^{-3}\mu m^2$; q*——channeling flow, $10^{-3}\mu m^2$; p_f——fracture pressure, MPa; p_f——matrix pressure, MPa; α——channeling coefficient, f; C_ρ——liquid compressibility, MPa^{-1}; C_Φ——rock compressibility, MPa^{-1}; C_t ——total compressibility, MPa^{-1}; G——Starting pressure gradient, MPa/m; γ——permeability modulus, MPa^{-1}; h——reservoir thickness, m; r_w——radius of the well, m; r_e——drainage radius, m; L——Length of model, cm; Δp—— Pressure difference, MPa; η——pseudo pressure, f. P_{Df} , P_{Dm} ——dimensionless pressure, dimensionless; r_D——dimensionless radius, dimensionless; λ——dimensionless channeling coefficient, dimensionless; t_D——dimensionless time, dimensionless; β——dimensionless fluid compressibility, dimensionless; γ_D——dimensionless permeability modulus, dimensionless; B—— dimensionless starting pressure gradient, dimensionless; ω——dimensionless elastic storage ratio, dimensionless; ζ——Laplace variable, dimensionless.

REFERENCES

[1] Miller RJ, Low PF. Threshold gradient for water flow in clay systems [J]. Soil Science Society of America Proceedings, 1963, 27 (6): 606 - 609.

[2] Feng Guoqing, Liu Qiguo, SHI Guang-zhi, etc. Considering the starting pressure gradient instability in low permeability gas reservoir seepage model [J]. Petroleum Exploration and Development, 2008, 35 (4): 457 - 461.

[3]Liu Jianjun, Liu X G., Hu Y R. vain low permeability rock Study on nonlinear seepage [J]. Rock Mechanics and Engineering, 2003, 22 (4): 556 - 561.

[4]Lizhong Feng, HE Shun-li low permeability oil reservoir boundary layer effects on the seepage law [J]. Petroleum Exploration and Development, 2005, 24 (2): 57 - 59, 77.

[5]Raghavan R. An Investigation by Numerical Methods of the Effeet of Pressure Dependent Roek and Fluid Properties on Well Flow Tests. PaPer SPE 2671,1969.

[6]Samaniego VF, Cineo-Ley H. On the Determination of the Pressure Dependent Characteristics of a Reservoir Through Transient Pressure Testing, Paper SPE19774, 1989:125 - 136.

[7]Pedrosa 0 A Jr. Pressure Transient Response in Stress-Sensitive Formations. Paper SPE 15115, 1986:213 - 221.

[8]Kikani.J., Pedr OA Jr. Perturbation Analysis of Stress - sensitive Reservoir. SPEFE, 1991, 6 (3): 379 - 386.

[9]Zhang MY, et al. New insights in Pressure-Transient Analysis for Stress-Sensitive Reservoirs. Paper SPE 28420, 1994.
[10]Gao Shusheng effective stress on hypotonic Porous Medium Parameters [J]. Liaoning Technical University: Natural Science, 2001, 20 (4).
[11]Yin Hongjun. Deformable medium reservoir seepage law and pressure characteristics of [J]. Hydrodynamics Research and Development (A Series), 2002, 17 (5): 538 - 546.
[12]Qin Ji Shun. Variable confining pressure low permeability sandstone storage Variation of permeability [J]. Xi'an Shiyou University (Natural Science Edition), 2002, 17 (4): 28 - 31.